Eur. J. Mech. B - Fluids 19 (2000) 707–722

S0997-7546(00)01094-3/FLA

On the receptivity of the by-pass transition to the length scale of the outer stream turbulence

Pavel Jonáš *, Oton Mazur, Václav Uruba

Department of Fluid Dynamics, Institute of Thermomechanics, Academy of Sciences of the Czech Republic, Dolejškova 5, 18200 Praha, Czech Republic

(Received 3 June 1999; revised 16 May 2000; accepted 23 May 2000)

Abstract – The effect of length scale on flat-plate by-pass boundary layer transition under free stream turbulence conditions has been investigated. Plane grids generated a constant value of 3 percent intensity turbulent fluctuations and five values of the dissipation length parameter in the range of 2.2 mm to 33.3 mm at 5 m/s flow velocity in the plane of the leading edge of the flat plate. The investigated boundary layer corresponds to the ERCOFTAC Test Case T3A+. Distributions of integral parameters as well as the statistical characteristics of the turbulent fluctuations were measured. They document a significant effect of turbulence length scale on the onset and the end of by-pass transition. It was found that the onset of the final stage of transition comes on later in 'fine-grained' turbulence than in the case of large free stream turbulence length scale. At the same time, the extent of the transition region shortens with decreasing length scale. Nevertheless, the transition process terminates sooner in a flow with a large turbulence length scale than in a flow with a small one. An attempt has been made to describe these observations quantitatively. © 2000 Éditions scientifiques et médicales Elsevier SAS

boundary layer / laminar-turbulent transition / by-pass transition / grid turbulence / turbulence scales

Nomenclature

C_f = skin friction coefficient
H_{12} = shape factor
Iu = longitudinal (streamwise) component of turbulent velocity fluctuations intensity
Iv = lateral (cross stream) component of turbulent velocity fluctuations intensity
L_e = dissipation length parameter
Re_2 = momentum thickness Reynolds number
U_e = mean free-stream (bulk flow) velocity
Var τ_w = variance of the wall shear stress fluctuations
u = fluctuating component of streamwise velocity
v = fluctuating component of cross stream velocity
x_G = distance of the grid upstream of the leading edge
δ_1 = displacement thickness
δ_2 = momentum thickness
γ = intermittency factor
λ_2 = lateral Taylor microscale

* Correspondence and reprints; e-mail: jonas@bivoj.it.cas.cz

ρ = density
τ_w = wall shear stress

Subscripts

e = in the outer flow
L = from the Blasius solution of laminar boundary layer flow
p = at the onset of the last stage (turbulent spots production) of transition
t = at the end of transition
T = from the Ludwieg and Tillmann skin friction coefficient formula
w = at the surface

1. Introduction

The prediction of transition location, both the onset of the process and the length of the region of laminar turbulent transition is of vital importance in many internal and external aerodynamic flow applications. The disparity of published transition observations is generally known (e.g. Loehrke et al. [1], Polyakov [2]). This is one of the reasons for the unsatisfactory accuracy of prediction methods (e.g. Savill [3]). In the last decade a number of meetings in Europe and the USA focused on the improvement of turbulence models for prediction of transition and relaminarisation, particularly in turbomachinery, have been dedicated to the solution of the problem (e.g. Savill [4], LaGraff and Ashpis [5]). It follows from the scatter of available data that the transition process is influenced by several factors, which are not entirely taken into account. Published surveys (e.g. Grek et al. [6], Mayle [7], Morkovin [8], Morkovin and Reshotko [9], Walker [10]) support this idea. The effect of the turbulence level of the incoming turbulent flow on laminar/turbulent transition is the most investigated factor in internal aerodynamic flows. However, there are reasons to expect that the length scale of the incoming flow turbulence, one of the neglected factors, will control the transition as well.

Why should the free stream turbulence length scale influence the laminar to turbulent boundary layer transition in addition to the intensity of fluctuations?

The common effect of length scale L_e and velocity scale $(\sqrt{\overline{u^2}})_e$ of the free stream turbulence is determined by:

- The fundamental features of the turbulence dynamics. From dimensional estimates it follows (e.g. Tennekes and Lumley [11]) that turbulent flow with a large length scale has a smaller rate of dissipation and decays less rapidly in the flow direction than 'fine grain' turbulent flow with shorter length scale. Therefore it obeys different decay laws in the mean flow direction. Consequently, the boundary layer on a rigid surface is perturbed in a different manner at any station downstream of the leading edge even if they reach the leading edge of the surface with the same mean flow and turbulence velocity scales.
- Wall constraint and the viscous limit at the surface for turbulence convected past a rigid wall moving with the mean flow velocity. Uzkan and Reynolds [12], Thomas and Hancock [13] and Hunt and Graham [14] have studied this problem. They found two layers at the surface that result from the wall constraint and the viscous limit at the surface. The first layer exhibits an outer kinematics region, extending up to a distance $\delta_0 \sim \Lambda$, where Λ is the integral length scale of the velocity fluctuations. The second layer – the inner viscous region – is affected also by viscosity in a zone of thickness $\delta_v \sim \sqrt{6/Re_T}\Lambda$, where Re_T is the turbulence Reynolds number. Both regions extend to distances normal to the surface which are

proportional to Λ. Important modifications of velocity component fluctuations from the state in the free stream originate in these regions so that disturbances affecting a thin boundary layer (thickness $\delta < \delta_0$) have different features than in the outer stream turbulence.

This effect has been ascertained in the framework of research on the turbulent boundary layer perturbed by free stream turbulence. It was predicted already in 1970, but only Hancock [15] proved it. His observations were supported in papers by Hancock and Bradshaw [16], Castro [17] and Jonáš [18]. It was shown that the effect of free stream turbulence on boundary layer characteristics might be described by means of a parameter containing both the free stream intensity, Iu_e, and the length scale, L_e. The parameter $F = aIu_e/(L_e/\delta + b)$ gives a more accurate and general correlation of characteristics than the intensity Iu_e alone. Empirical constants a, b have values: $a = 1$, $b = 2$ or $a = 2$, $b = 5$ according to [15] or [17]. As the turbulent boundary layer is the result of the transition process, the intensity Iu_e and the length scale L_e must influence the process.

The main aim of the investigations made in the Institute of Thermomechanics (IT) Academy of Sciences of the Czech Republic (AS CR) was to document the effect of the turbulence length scale on the onset and on the development of laminar/turbulent transition in a flat plate boundary layer. The goal was also to generate experimental results that would serve as Test Case T3A+ defined by the COST/ERCOFTAC Special Interest Group on Transition (e.g. Savill [4]).

2. Experimental facility and measurement technique

The working section (cross section: 0.5×0.9 m^2, length 2.69 m) of the closed circuit wind tunnel of the IT AS CR has been rebuilt to make possible comparative investigations of the flat-plate boundary layer transition with grid turbulence. In *figure 1*, the schematic of the test section is shown and the orthogonal co-ordinate system (x, y, z) is introduced. The boundary layer develops on an aerodynamically smooth plate 2.75 m long and 0.9 m wide. The plate is made from a laminated wood-chip board 25 mm thick. Three methods are applied to prevent flow separation at the leading edge and to remove circulation around the plate:

- small change of the angle of attack of the plate as a whole;
- a deflected full span flap; and
- a screen placed across the flow in the upper part of the working section a bit upstream of the flap.

The shape of the cylindrical leading edge has been designed and examined by Kosorygin et al. [19]. Only a part of the plate, 1.62 m in length, lies in the test section with very slight divergence. The remaining part is situated in the wind tunnel diffuser ($\sim 6°$).

The schematic in *figure 1* shows the location of grid turbulence generators upstream of the plate. A family of square mesh plane grids/screens was developed. (Jonáš [20]). They generate homogeneous, close to isotropy, turbulence with 'prescribed' intensity Iu_e and with the grid related length scale L_e in the plane $x = 0$. The control of the generated turbulence is established by various dimensions (diameter of cylindrical rods d and mesh M) and by the proper distance upstream of the leading edge, $x = x_G < 0$, at which the individual grids are placed. *Table I* summarises the important characteristics of the grid turbulence generators used.

All measurements were carried out by means of two hot-wire probes working in constant temperature anemometry (CTA) mode:

- the first probe, with a single wire, is in a fixed position in the outer stream;
- the second probe – the 'profile probe', a single wire or X-type probe, is driven by a traversing system in the streamwise direction x and in the direction y normal to the surface. The distance y from the wall of the hot wire of the 'profile probe' is measured with an accurate cathetometer.

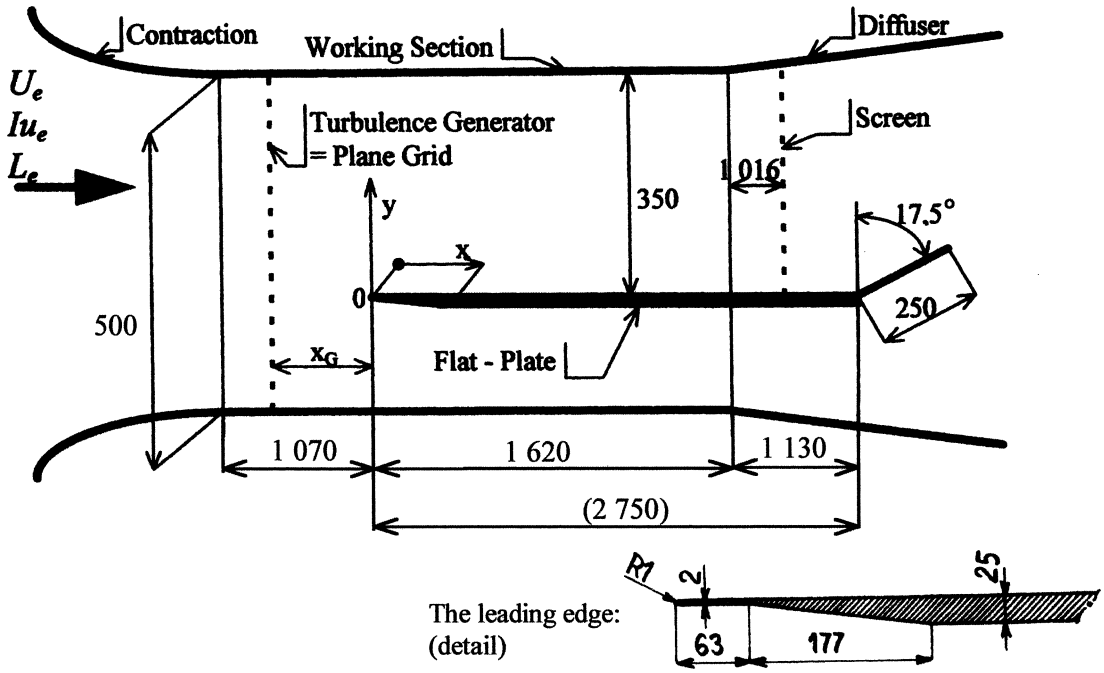

Figure 1. Working section of the wind tunnel (0.5×0.9) m^2.

Table I. Turbulence generators.

Designation	d [mm]	M [mm]	Porosity [%]	x_G [m]
GT1	3	20	72	−0.445
GT3	6	40	72	−1.087
GT3 (retry)	6	40	72	−1.076
GT5	10	35	51	−1.350
GT8	1.65	5.75	51	−0.194
GT9	1	5	64	−0.123

A sequence of at least 16 sections $x = x_i$(constant) < 1.95 m $(i = 1, 2, \ldots, 16, \ldots)$ was investigated downstream of each turbulence generator.

The anemometers (DANTEC 55M and 56N systems) and the traversing system (DANTEC 57H00) are controlled by a personal computer Pentium EISA 133 MHz. The computer is equipped with a National Instruments (EISA A-2000) Data Acquisition System and controlled by LabVIEW software. An accurate DC digital voltmeter (HP 34970A) is used to determine the mean values (averaging of the repeated readings) of the output signals of both CTA channels. Together with the voltmeter measurement the output signal of the profile probe is digitally recorded (sampling rate 25 kHz; 12 bit; variable offset-voltage) and evaluated subsequently. The length of records is from 30 s to 60 s.

A special calibration set up with a metering nozzle has been developed to provide high accuracy of the hot-wire calibration in the range of 0.3 to 10 m/s. The nozzle output orifice has an area only 0.1 of the area of the section in which the wire is calibrated. The calibration of each probe was repeated after 2–3 hours exposure in the stream.

(1) The evaluation of measurements proceeds in the following steps: Transformation of recorded electric signal onto an array of samples of instantaneous velocity that is performed by means of the generalised Collis-Williams cooling law (e.g. Bradshaw [21]); and the directional sensitivity formula of Hinze [22]

$$Nu\left(\frac{T_{\mathrm{m}}}{T}\right)^{M^*} = A + B\,Re^N; \quad Nu \sim E^2;\ Re \sim U_{\mathrm{eff}};\ U_{\mathrm{eff}}^2 = \bar{U}^2\left(1+\kappa\cos^2\varphi\right), \tag{1}$$

where A, B, M^*, N and κ are individual empirical parameters of each hot wire; the customary definitions of Nusselt and Reynolds numbers are introduced; φ is the angle between the wire and the stream direction; U_{eff} is the effective value of the mean flow velocity $\bar{U}$.

(2) Correction of the hot wire reading near the surface to remove wall proximity effect on the cooling of the hot-wire. The correction procedure applied is described in detail by Jonáš et al. [23]. It consists of linear regression of the mean velocity profile close to the wall. The absolute term of the regression corrects the zero error in reading the hot-wire starting position close to the wall. The slope of the regression yields the derivative $(\mathrm{d}\bar{U}/\mathrm{d}y)_{\mathrm{w}}$ of the mean velocity normal to the wall at the wall $(y = 0)$, so that together with the wall-proximity correction the mean value of the wall shear stress $\bar{\tau}_{\mathrm{w}}$ is determined.

(3) Evaluation of wall-friction fluctuations from the records of hot-wire measurements of velocity profiles. A special procedure was developed [23] for this purpose. Thus it is possible to determine the distributions of some statistical characteristics of the wall friction during the transition process. Only the development of the variance of wall shear stress fluctuations τ'_{w} will be discussed in this paper

$$\mathrm{Var}\,\tau_{\mathrm{w}} = \overline{\left(\tau'_{\mathrm{w}}\right)^2}. \tag{2}$$

(4) Evaluation of statistical characteristics of the velocity fluctuations following the rules of mathematical statistics. The following expressions are used:

- the intensities Iu and Iv of turbulent fluctuations of streamwise, u, and lateral, v, components of the stream velocity are given as:

$$Iu = \sqrt{(\overline{u^2})}/\bar{U} \quad \text{and} \quad Iv = \sqrt{(\overline{v^2})}/\bar{U}; \tag{3}$$

- the dissipation length parameter taken after Hancock and Bradshaw [24]

$$L_{\mathrm{e}} = -(\overline{u^2})_{\mathrm{e}}^{3/2}/\bar{U}_{\mathrm{e}}\frac{\mathrm{d}(\overline{u^2})_{\mathrm{e}}}{\mathrm{d}x} \tag{4}$$

Table II. Important features of flow in the neighbourhood of the plane $x = 0$.

Grid	Iu_{e} [%]	$(\frac{Iv}{Iu})_{\mathrm{e}}$ [1]	$(\frac{\overline{uv}}{U^2})_{\mathrm{e}}$ [1]	L_{e} [mm]	C [1]	m [1]	$\frac{x_0}{M}$ [1]
GT1	3.0	1.02	$-2.0.10^{-5}$	5.9	146.9	0.910	−8.7334
GT3	3.0	1.05	$-2.1.10^{-5}$	15.9	9.8986	1.563	−20.574
GT3 (retry)	3.0	1.05	$-2.1.10^{-5}$	15.3	12.841	1.514	−19.212
GT5	3.0	1.03	$-1.6.10^{-5}$	33.3	0.2987	1.985	−64.893
GT8	3.0	∼1	$\sim 10^{-5}$	3.8	17.556	1.249	−28.114
GT9	3.0	∼1	$\sim 10^{-5}$	2.2	16.252	1.412	−21.006

is computed by means of an empirically determined decay law of turbulence energy given as

$$Iu^{-2} = C\left(\frac{x}{M} - \frac{x_0}{M}\right)^m, \tag{5}$$

where M is the span of cylindrical rods of a plane grid with squared meshes;

- the lateral dissipation length scale (Taylor microscale) λ_2 derived from the auto-correlation function applying Taylor's assumption and with regard to satisfactory isotropy of fluctuations (see *table II*) and
- the Reynolds number of outer stream turbulence is

$$Re_T = \lambda_2 \sqrt{(\overline{u^2})_e}/\nu. \tag{6}$$

3. Measurement uncertainties

The experimental uncertainties are estimated based on knowledge of instrumentation, calculated root mean square errors of interpolations and taking into account the spread of repeated observations.

The estimated probable error of the mean velocity $\bar{U}$ is less than 0.3 percent. The error estimates for intensities of turbulent velocity fluctuations Iu and Iv are about 3 percent. The uncertainty of the measurement of successive shifts of the profile probe is less then 0.01 mm, however the possible error in reading the initial hot wire position y_1 might be up to $y_0 = 0.05$ mm. In the course of correcting for the effect of wall proximity, the error of reading the initial hot wire distance from the wall is corrected $(+/-0.01$ mm) and the derivative $(\mathrm{d}\bar{U}/\mathrm{d}y)_W$ at the wall is determined with a relative error of about 2 percent on average. The uncertainties of microscale λ_2 and dissipation length parameter L_e are estimated as up to 6 percent. Consequently, possible errors have been derived in the determination of the Reynolds number of outer stream turbulence Re_T (less than 10%), shape factor H_{12} (about 3%) and intermittency factor γ (about 5%).

4. Boundary conditions

Boundary conditions for the investigated boundary layers were set up experimentally to fulfil the requirements of Test Case T3A+ by the COST/ERCOFTAC Special Interest Group on Transition/Re-transition (e.g. Savill [4]):

(a) mean velocity $U_e = 5$ m/s, constant over the test surface;

(b)turbulence intensity $Iu = 3\%$ at the flat-plate leading edge $x = 0$; and

(c)various turbulence length scales L_e at $x = 0$.

Throughout the whole experimental program the requirement (a) has been fulfilled with departures between measurements of individual profiles less than 2 percent but the oscillation throughout the measurement of a single profile is less than 0.3 percent. It should be noted that only 1.62 m of the total length of the plate lies in the working section with cross section (0.9×0.5) m^2. As a result, the free stream mean velocity U_e is constant and equal to the value in the leading edge plane $x = 0$ (within the limits of measuring accuracy $\pm 0.5\%$) until $x = 1.62$ m only. Farther downstream, the plate is in a decelerating flow and the free stream mean velocity decreases to $0.96\,U_e$ at $x = 2$ m. The value of the pressure gradient parameter is estimated there as

$$F = \frac{\delta_2}{U_e}\frac{\mathrm{d}U_e}{\mathrm{d}x} \sim 3.6 \cdot 10^{-4}. \tag{7}$$

This might slightly accelerate the transition process unless it is terminated sooner.

The flow near the leading edge has been examined to exclude any occurrence of flow separation in the neighbourhood of the leading edge. The check was done directly by means of the liquid-film method. An additional indirect examination is the comparison of the measured mean velocity profiles $\bar{U}/U_e$ with the Blasius solution $F'(\eta)$. An example is shown in *figure 2* which displays plotted profiles of the dimensionless mean velocity (vertical axis) against the Blasius function (horizontal axis). The value of the Blasius variable η is calculated using the formula $\eta = 0.664y/\delta_2$; the momentum thickness $\delta_2(x)$ is derived from measurements. It is evident that the measured profiles are in good agreement with the Blasius profile close to the leading edge of the plate ($x \leqslant 0.2$ m) before the beginning of the transition (intermittency factor $\gamma = 0$; see section 6.)

The most important features of turbulent flow in the neighbourhood of the plane $x = 0$, downstream of the turbulence generators, are summarised in *table II*. The parameters of the decay law, C, m and x_0, are derived from the distributions of the intensity of longitudinal velocity component fluctuations in the range $\langle x_a, x_b \rangle$ given by

$$x_a \approx x_G + 15M \geqslant -0.15\,\text{m}; \qquad x_b \approx x_G + 60 \div 100M,$$

and at a distance $y = 0.1$ m above the plate. The distributions have been interpolated by formula (5).

Farther downstream, the decay of turbulence fluctuations decelerates and at least, for $x > 0.8$ m in the finest grain turbulence (GT8 and GT9), the fluctuations begin to amplify. Distributions of the intensity Iu_e along the plate at a distance $y = 0.1$ m from the wall are shown in *figure 3*. They show that the intensity Iu_e in each type of generated turbulence is the same in the plane $x = 0$; but that the rates of dissipation of the turbulence energy are different. Arrows with relevant symbols indicate values of turbulence intensity at the onset and end of transition in *figure 3*.

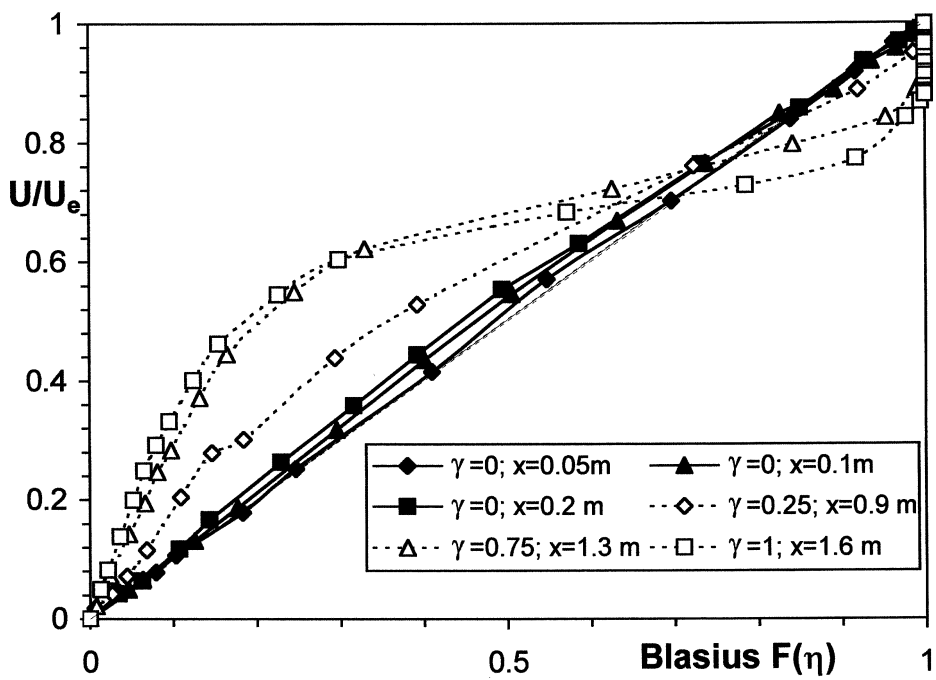

Figure 2. Comparison of measured mean velocity profiles with the Blasius profile ($L_e = 5.9$ mm at $x = 0$).

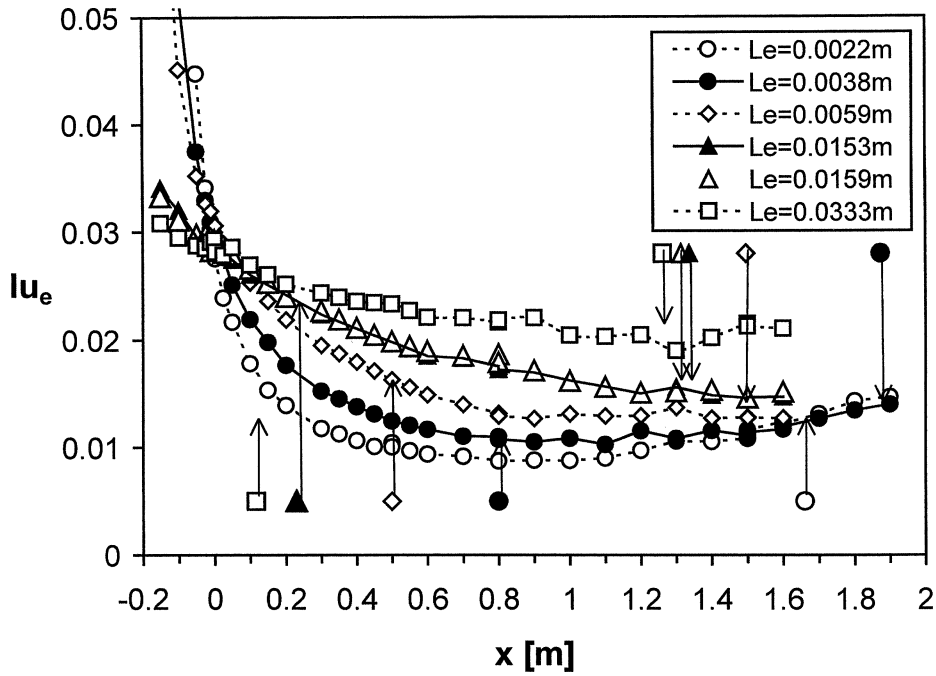

Figure 3. Distributions of the intensity Iu_e along the plate at a distance $y = 0.1$ m from the wall (L_e at $x = 0$). Arrows with relevant symbols indicate values at the onset and at the end of transition.

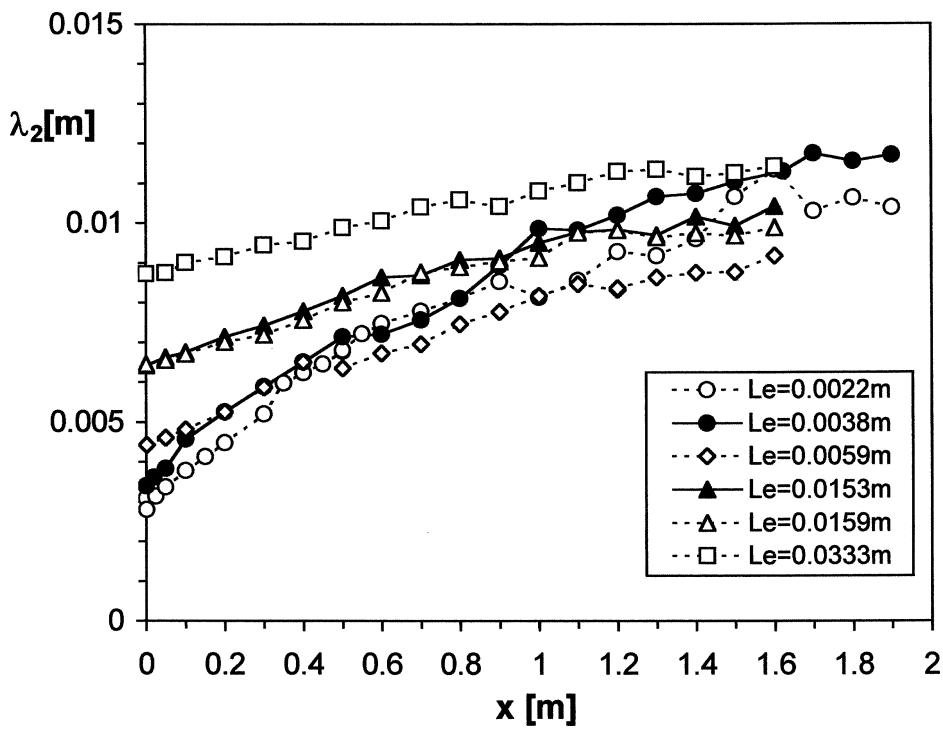

Figure 4. Distributions of the Taylor lateral microscale outside the boundary layer (L_e at $x = 0$).

The distributions of the Taylor lateral microscale λ_2 are displayed in *figure 4*. They show that the length scales of the turbulence disturbances differ by one order of magnitude at the leading edge plane. However, all distributions of Taylor microscale tend to come together with increasing x.

5. Mean velocity profiles

The distributions of the fundamental boundary layer characteristics have been established on the basis of detailed mean velocity profile measurements. Comparison of the measured mean velocity profiles with the Blasius profile (*figure 2*) illustrates the dramatic evolution of the profile shape, especially after the onset of transition, i.e. the beginning of turbulent spot formation accompanied with a departure of the mean flow parameter distributions from their laminar boundary layer counterparts (intermittency is still $\gamma = 0$). The semi-logarithmic plots of mean velocity profiles (*figure 5*) confirm this observation and, in addition, indicate that the viscous sublayer appears thicker than might be seen usually. Also the value of the constant in the law of the wall becomes affected in this case. These properties imply (e.g. Huffman and Bradshaw [25]) that the local momentum thickness Reynolds number Re_2 is low – often less than 1000 and at most 1400. After the end of transition, the mean velocity profiles approach the shape typical of a turbulent boundary layer (intermittency attains the value $\gamma = 1$). The semi-logarithmic plots are providing an indirect test of the accuracy of the evaluation of the wall shear stress.

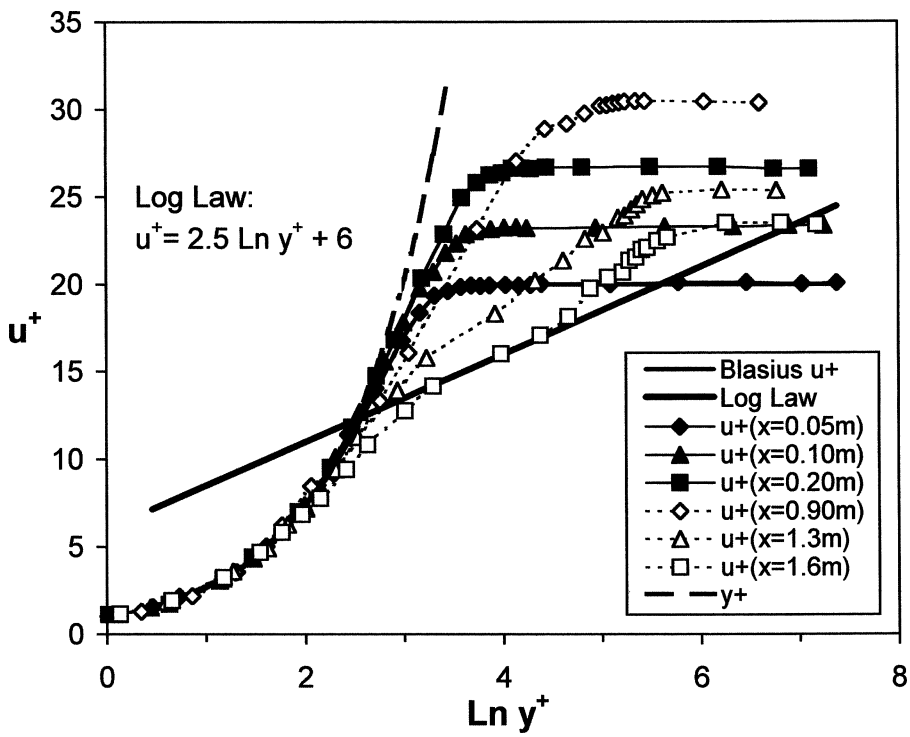

Figure 5. Semi-logarithmic plots of mean velocity profiles ($L_e = 5.9$ mm at $x = 0$; wall-units).

6. Fundamental boundary layer characteristics

The fundamental boundary layer characteristics, thicknesses of various kinds, shape factor H_{12}, skin friction coefficient C_f and intermittency factor γ (Emmons [26]) were evaluated from the mean velocity profiles.

In *figure 6*, the shape factor's distributions as a function of the distance x from the boundary layer origin are plotted. The value of $H_{12} = 2.6$ is in accordance with the Blasius solution of a laminar boundary layer in the region quite near to the leading edge of the plate. The shape factor begins to fall usually prior to the start of transition. *Figure 6* shows the shift of the shape factor distributions in the streamwise direction with decreasing length scale parameter L_e. The minimum value of $H_{12} = 1.45$ is attained after termination of the process. The value is higher than expected following published data (~ 1.3) but the Reynolds number Re_2 of our experiment was low indeed ($Re_2 \leqslant 1400$, see *figure 8*).

The distributions of the skin friction coefficient along the plate in the boundary layers are shown in *figure 7* together with the distributions $(C_f)_L$ and $(C_f)_T$ corresponding to Blasius (laminar boundary layer) and Ludwieg and Tillmann (turbulent boundary layer; e.g. Schlichting [27]). These distributions show that the region of transition is moving downstream with decreasing length scale of turbulence, though the turbulence intensity in the leading edge plane, $x = 0$, is equal to 3 percent downstream of each turbulence generator. In addition, it is evident that the end of the transition process has not been reached in the flow downstream of the finest grid generator (GT9) as the length of the working section of the wind tunnel is too short.

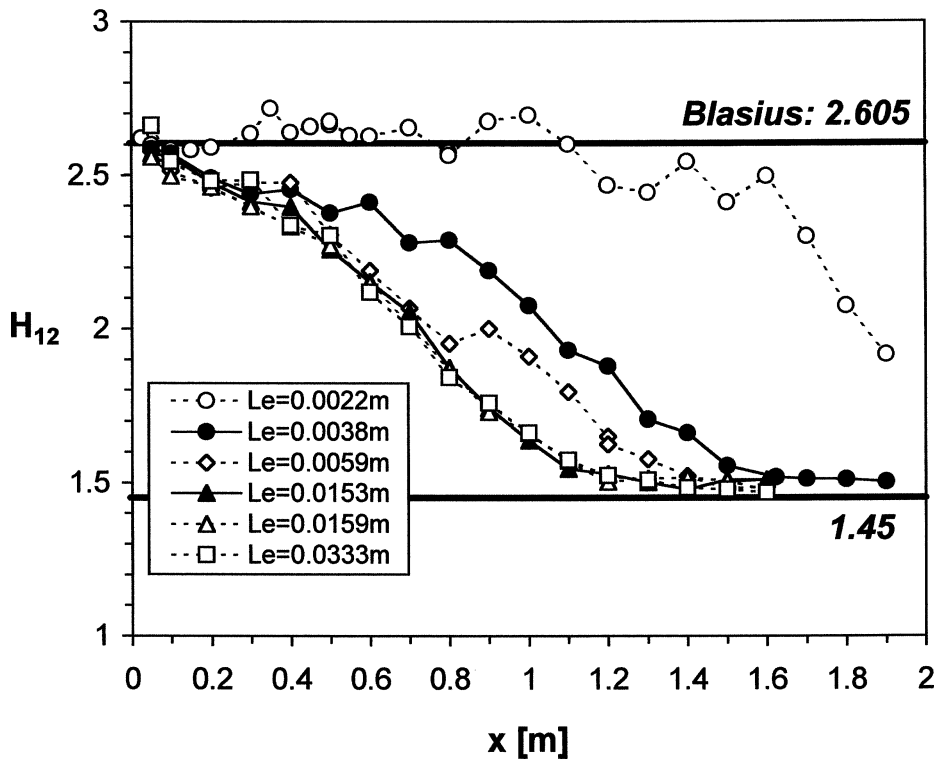

Figure 6. Distributions of the shape factor (L_e at $x = 0$).

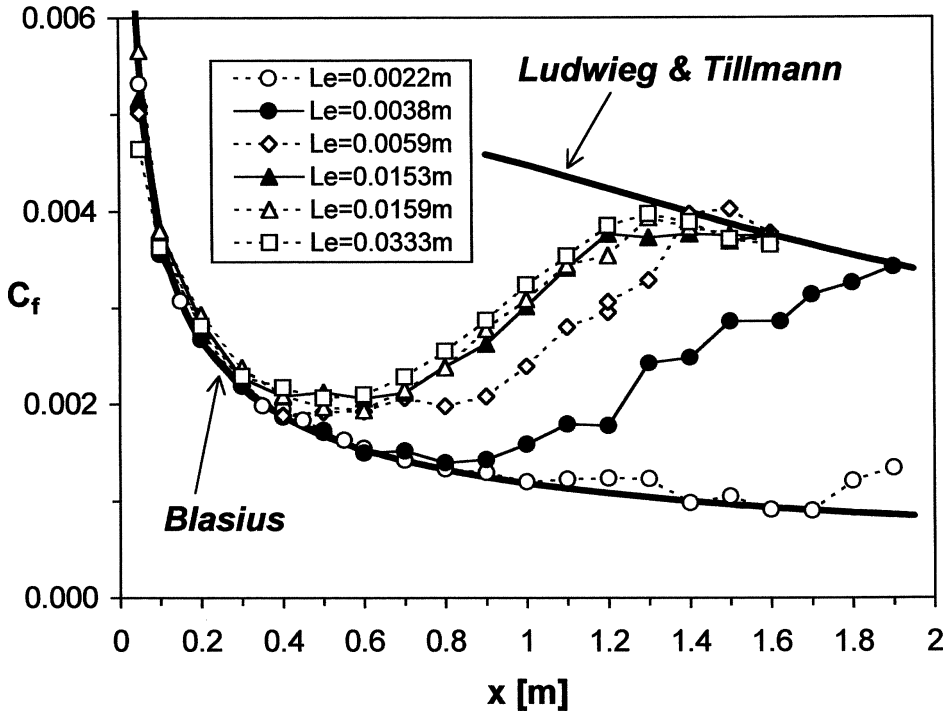

Figure 7. Distributions of the skin friction coefficient (L_e at $x = 0$).

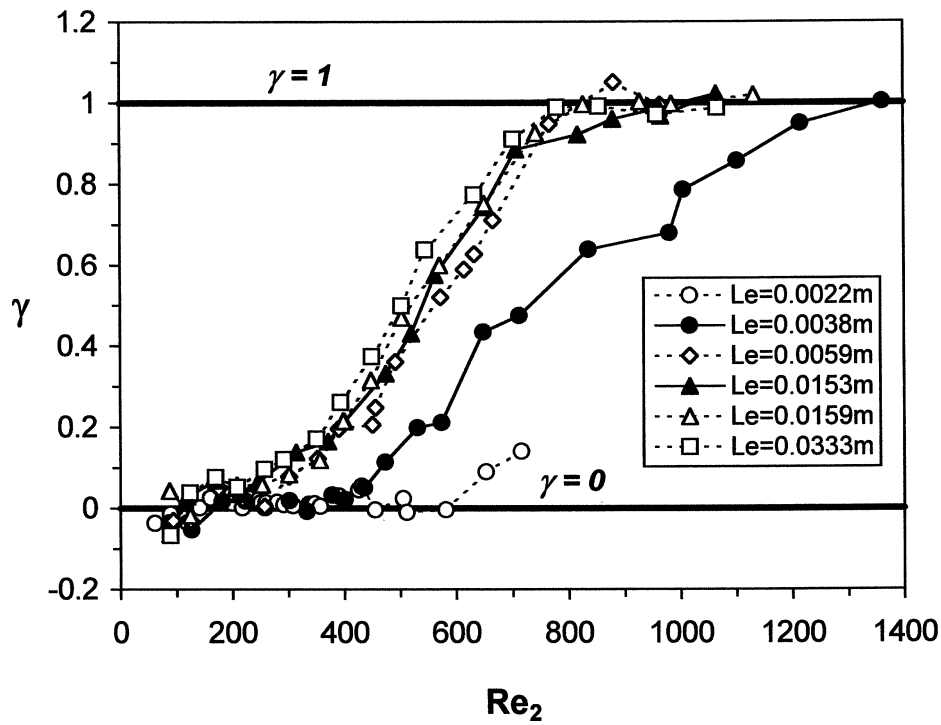

Figure 8. Distributions of the intermittency factor (L_e at $x = 0$).

Some current transition models apply an intermittency correlation to handle transition. Following Emmons' concept [26], the data presented are computed using the definition of the intermittency factor γ

$$C_f(Re_2) = (1-\gamma)(C_f)_L + \gamma(C_f)_T. \tag{8}$$

The laminar and turbulent values, $(C_f)_L$ and $(C_f)_T$, are computed at the local value of the momentum thickness Reynolds number Re_2. The distributions of the factor γ as a function of the Reynolds number Re_2 are shown in *figure 8*. They confirm the distinct effect of turbulence length scale on by-pass transition. They show that the region of transition is moving downstream with the decreasing length scale of turbulence.

7. Wall friction fluctuations during transition

It was observed that the distinctive regions of the boundary layer transition process are most pronounced in the distribution of the skin friction coefficient C_f. We expect that the wall shear stress fluctuations will reflect the evolution of the flow structure. This should appear in the distributions of statistical characteristics of the wall-friction fluctuations. Their analysis can help to increase the accuracy of the location of the important stages of the transition process and to refine the notion of variation of the wall friction fluctuations. The onset and the end of transition are well distinct from the distribution of the variance of wall-friction shown in *figure 9*.

A region of constant variance $\mathrm{Var}\,\tau_w$ precedes the onset (left arrows in *figure 9*). The subsequent large increase of $\mathrm{Var}\,\tau_w$ is terminated upstream of the position estimated as the end of transition (right arrows in *figure 9*) from the C_f distribution. The curves, describing measurements downstream of individual turbulence generators, differ in slope considerably. The slope displays the rapidity of transition to turbulence. The values of $\mathrm{Var}\,\tau_w$ are very similar in all investigated boundary layers before the transition starts. It is hard to dismiss

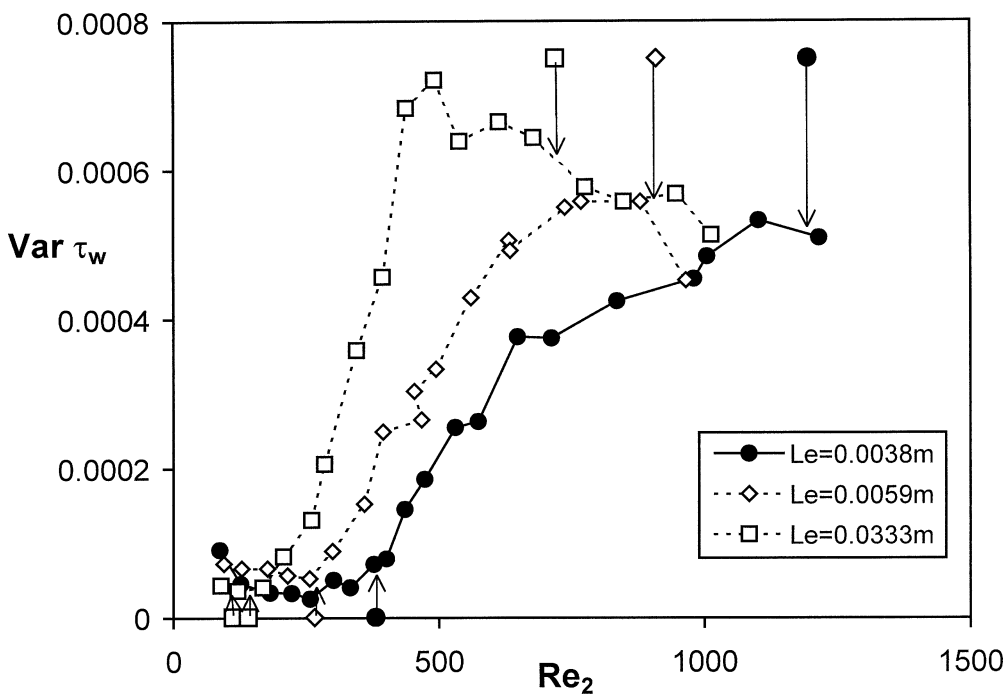

Figure 9. Distributions of the variance of wall-shear stress (L_e at $x = 0$). Arrows as in *figure 3*.

the idea that the value of $\mathrm{Var}\,\tau_w$ is independent of the local intensity and length scale until the transition starts. Similarly, the variance $\mathrm{Var}\,\tau_w$ seems to be independent of the local momentum thickness Reynolds number Re_2 after termination of the transition process. Undoubtedly, the effect of the length scale on transition onset and its speed are very distinct from the plots of variance of the wall friction fluctuations.

8. Preliminary correlation of transition Reynolds number

The values of the Reynolds numbers Re_x and Re_2 at the onset (subscript 'p') and at the end (subscript 't') of the transition region can be determined from the distribution of integral properties of the transitional boundary layers investigated. The first attempt to correlate these Reynolds numbers with the dissipation length parameter is described in Jonáš et al. [28]. The analysis of the distributions of the variance of wall shear stress fluctuations adds precision to it.

The momentum thickness Reynolds numbers corresponding to the onset, $(Re_2)_p$ and to the end, $(Re_2)_t$, of transition for the investigated boundary conditions are plotted as functions of the dissipation length parameter in *figure 10*. Measurement at $L_e = 0.0333$ m of the onset of transition was repeated after the wind tunnel reconstruction. Both results are plotted in *figure 10* (square symbols) to indicate the reproducibility of the experiments described. In spite of the small number of interpolated points, the regression curves have been determined

$$(Re_2)_p = \left(\frac{245}{L_e}\right)^{0.535}, \quad r^2 = 0.997, \tag{9}$$

$$\frac{(Re_2)_t - (Re_2)_p}{(Re_2)_p} = 1.7427 + 108L_e, \quad r^2 = 0.998, \tag{10}$$

where r denotes the correlation coefficient.

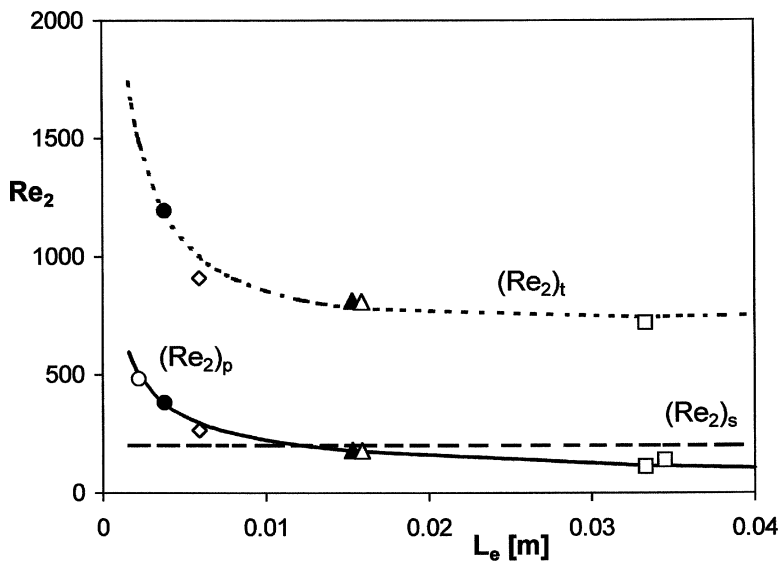

Figure 10. Momentum thickness Reynolds number at the onset and the end of transition (L_e at $x = 0$). Symbols as in *figure 3*.

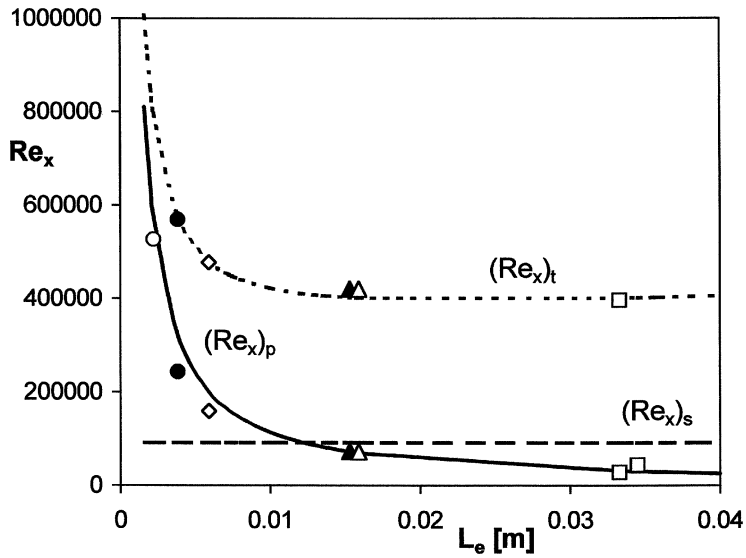

Figure 11. Local Reynolds number at the onset and the end of transition (L_e at $x = 0$). Symbols as in *figure 3*.

The minimum critical momentum thickness Reynolds number on the neutral curve, $(Re_2)_s = 201$, computed by Wazzan et al. [29] (see also [30], page 405), is also shown in *figure 10*. It appears that the onset value $(Re_2)_p$ for larger length scales, can be even smaller than the minimum critical value $(Re_2)_s$.

The variations of the local Reynolds numbers corresponding to the minimum critical Reynolds number and to the onset and end of the laminar/turbulent transition are shown in *figure 11*. Regression equations have been derived in the forms

$$(Re_x)_p = \left(\frac{526}{L_e}\right)^{1.071}, \quad r^2 = 0.999, \tag{11}$$

$$\frac{(Re_x)_t - (Re_x)_p}{(Re_x)_p} = 2520 L_e (Re_x)_p^{-0.19}, \quad r^2 = 0.998. \tag{12}$$

It should be recalled that the regressions (9)–(12) are valid for boundary conditions described in section 4 only.

9. Conclusions

The experiments described here show that the length scale of turbulence in the incoming flow influences the beginning and extent of the transition region. Correlations of Reynolds numbers corresponding to the onset and termination of by-pass transition at the investigated boundary conditions yield the following conclusions:

- The onset of by-pass transition moves downstream with decreasing length scale of turbulent disturbances at a fixed intensity of turbulent fluctuations in the leading edge plane – the laminar part of the boundary layer becomes longer.
- The transition region becomes shorter.
- Nevertheless, the transition process terminates earlier in flow with larger turbulence length scale than in flow with a smaller value of it.

A comparison of experimental results with predictions using empirical models proposed by Abu Ghannam and Shaw [31], Fasihfar and Johnson [32] and Mayle [33] for the transition onset is shown in *figure 12*. The values of the momentum thickness Reynolds number $(Re_2)_p$ corresponding to the onset of transition are plotted as functions of turbulence intensity at the origin of the boundary layer $Iu = 0.03$ (right symbols) and as functions of the local intensity $Iu(x_p)$ at the location x_p where the transition process begins. Evidently, a transition prediction based on turbulence intensity in the leading edge plane, $x = 0$, fails.

As is apparent from *figure 12*, the local turbulence intensity alone is not sufficient to describe transition. Though being of much less significance the length scale or the dissipation rate also contribute to transition control, similarly to the effect of free stream turbulence in a turbulent boundary layer (see Introduction).

Further experiments are necessary to explain this problem and to develop correlations of more general validity than correlations (equations (9) to (12)) which are of limited importance as they are derived from experiments restricted to the COST/ERCOFTAC Test Case T3A+ only. However, those presented here can serve as an illustration of the effect of the length scale on by-pass transition, and can be used in the development of mathematical models of transitional boundary layers.

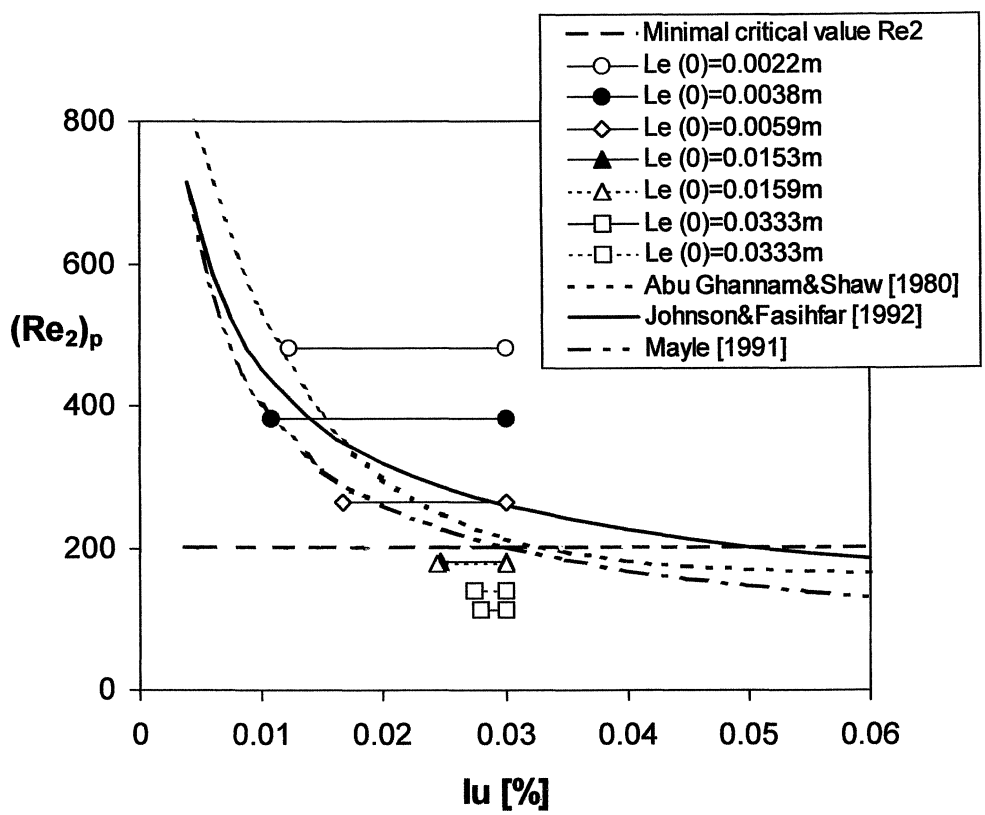

Figure 12. Comparison of the transition onset results with prediction of empirical models.

Acknowledgements

The authors gratefully acknowledge the support received from the government of the Czech Republic via the Ministry of Education Youth and Physical Training of CR (COST Project No. OC.F1.10) and from the Grant Agency of the Czech Republic (Projects No. 101/98/K001 and No. 101/00/1057).

References

[1] Loehrke R.I., Morkovin M.V., Fejer A.A., Review – Transition in nonreversing oscillating boundary layers, J. Fluid. Eng-T. ASME 97 (1975) 534–549.
[2] Polyakov N.F., The influence of the low-free-stream perturbations on the condition of laminar boundary layer, Arch. Mech. Stosowaney 31 (1979) 327–338.
[3] Savill A.M., Some recent progress in the turbulence modelling of by-pass transition, in: So R.M.C., Launder B.E. (Eds.), Near-wall turbulent flows, Elsevier, Amsterdam, 1993, pp. 829–848.
[4] Savill A.M., COST-ERCOFTAC transition SIG COST action workshop IT AS CR Prague, ERCOFTAC Bulletin No. 25 (1995) 36–37.
[5] LaGraff J.E., Ashpis D.E. (Eds.), Minnowbrook II – 1997 workshop on boundary layer transition in turbomachines, Proceedings of a workshop held at the Minnowbrook Conference Center, Syracuse University, Syracuse, New York, September 7–10, 1997, NASA Lewis Research Center, NASA/CP – 1998–206958, Cleveland, 1998.
[6] Grek G.R., Kozlov V.V., Ramazanov M.P., Laminar-turbulent transition under turbulized incoming flow, Sibir. Phys.-Techn. J. 6 (1991) 106–137 (in Russian).
[7] Mayle R.E., The role of laminar-turbulent transition in gas turbine engines, J. Turbomach. 113 (1991) 509–537.
[8] Morkovin M.V., By-pass transition research: Issues and philosophy, in: Proc. Symposium for Eli Reshotko 60th Anniversary, Springer-Verlag, Berlin, 1992, pp. 1–24.
[9] Morkovin M.V., Reshotko E., Dialogue on progress and issues in stability and transition research, in: Arnal D., Michel R. (Eds.), Laminar-turbulent transition, Springer-Verlag, Berlin, 1990, pp. 3–29.
[10] Walker G.J., The role of laminar-turbulent transition in gas turbine engines: A discussion, ASME Paper 92-GT-301, 1992.
[11] Tennekes H., Lumley J.L., A First Course in Turbulence, MIT Press, Cambridge, MA, 1974.
[12] Uzkan T., Reynolds, W.C., A shear-free turbulent boundary layer, J. Fluid Mech. 28 (1967) 803–821.
[13] Thomas N.H., Hancock P.E., Grid turbulence near a moving wall, J. Fluid Mech. 82 (1977) 481–496.
[14] Hunt J.C.R., Graham J.M.R., Free-stream turbulence near plane boundaries, J. Fluid Mech. 84 (1978) 209–235.
[15] Hancock P.E., The effect of free stream turbulence on turbulent boundary layers, Ph.D. thesis, Imperial College, Univ. of London, 1980.
[16] Hancock P.E., Bradshaw P., The effect of free stream turbulence on turbulent boundary layers, J. Fluid. Eng-T. ASME 105 (1983) 284–289.
[17] Castro I.P., Effects of free stream turbulence on low Reynolds number boundary layers, J. Fluid. Eng-T. ASME 106 (1984) 298–306.
[18] Jonáš P., On turbulent boundary layer perturbed by outer flow turbulence, Power Eng. Journal, No. 43, Academia, Vilnius, Lithuania (1992) 69–80.
[19] Kosorygin V.S., Levchenko V.Ja., Polyakov N.F., On problem of the origin of waves in a laminar boundary layer, Preprint ITPM, No.12–82, ITPM SO AN SSSR, Novosibirsk, 1982 (in Russian).
[20] Jonáš P., Control of free-stream turbulence by means of passive devices, in: Proc. of International Seminar 'Problems of Simulation in Wind-Tunnels', Pt.2, ITPM SO AN SSSR, Novosibirsk, 1989, pp. 160–174.
[21] Bradshaw P., An Introduction to Turbulence and Its Measurement, 1st ed., Pergamon Press, Oxford, 1971.
[22] Hinze J.O., Turbulence, 2nd ed., McGraw-Hill, New York, 1975.
[23] Jonáš P., Mazur O., Uruba V., Statistical characteristics of the wall friction in a flat plate boundary layer through by-pass transition, Z. Angew. Math. Mech. 79 (1999) S691–S692.
[24] Hancock P.E., Bradshaw P., Turbulence structure of a boundary layer beneath a turbulent free stream, J. Fluid Mech. 205 (1989) 45–76.
[25] Huffman G.D., Bradshaw P., A note on von Karmán's constant in low Reynolds number turbulent flows, J. Fluid Mech. 53 (1972) 45–60.
[26] Emmons H.W., The laminar turbulent transition in boundary layer, J. Aero. Sci. 18 (1951) 490–498.
[27] Schlichting H., Grenzschicht Theorie, 3rd ed., G. Braun, Karlsruhe, 1958.
[28] Jonáš P., Mazur O., Uruba V., Experiments on by-pass boundary layer transition with several turbulence length scales, in: IMechE Conference Transactions, Vol. A, London, 1999, pp. 179–188.
[29] Wazzan A.R., Keltner G., Okamura T.T., Smith A.M.O., McDonnell-Douglas Co. Rep. DAC-67086, 1968.
[30] White F.M., Viscous Fluid Flow, McGraw-Hill, New York, 1974.
[31] Abu Ghannam B.J., Shaw R., Natural transition of boundary layers – The effects of turbulence, pressure gradient and flow history, J. Mech. Eng. Sci. 22 (5) (1980) 213–228.
[32] Fasihfar A., Johnson M.W., An improved boundary layer transition correlation, ASME paper 92-GT-245, 1992.
[33] Mayle R.E., The role of laminar-turbulent transition in gas turbine engines, J. Turbomach. 113 (1991) 509–537.